International Journal of Materials Science

E-ISSN: 2707-823X
P-ISSN: 2707-8221
IJMS 2021; 2(2): 01-07
Received: 02-10-2021
Accepted: 10-11-2021

Sanjay Kumar Dubey
Department of Physics, Kalinga University, Naya Raipur, Chhattisgarh, India

Shashank Sharma
Department of Physics, Kalinga University, Naya Raipur, Chhattisgarh, India

AK Diwakar
Department of Physics, Kalinga University, Naya Raipur, Chhattisgarh, India

Corresponding Author:
Shashank Sharma
Department of Physics, Kalinga University, Naya Raipur, Chhattisgarh, India
Email: dr.shashankeinstein@rediffmail.com

Synthesization of $Ba_2MgSi_2O_7$: Eu^{2+}, Dy^{3+} phosphor by combustion route and their characteristics

Sanjay Kumar Dubey, Shashank Sharma and AK Diwakar

Abstract
$Ba_2MgSi_2O_7$: Eu^{2+}, Dy^{3+} phosphor was synthesized by combustion reaction technique. Phase identification was done by X-ray diffraction analysis and its results revealed monoclinic structure with a space group C2/c. This structure is a member of melilite group. The average crystallite size (D) is calculated as 29.10 nm and lattice strain as 0.30. The functional group identification of this phosphor with the help of FTIR spectroscopy. When the $Ba_2MgSi_2O_7$:Eu^{2+}, Dy^{3+} phosphor was excited with 395nm wavelength single broad emission peak situated at 520 nm was obtained. PL and CIE chromaticity diagram clearly indicates that the bright green emission was observed near UV region. Thermo-luminescence (TL) of the UV-irradiated (254 nm) samples was recorded with the help of routine TL set-up Nucleonix TLD reader with constant heating rate 5^0Cs^{-1}. The optimum TL intensity assigned at 100.12 ^oC temperature and displays single TL glow curve peak. The favorable features for applications likewise near UV-LED conversion phosphor, Image processing of computer science and found their considerable persistency etc. In this present paper, XRD, FTIR, PL, CIE Chromaticity Diagram, TL properties of the phosphor also reported.

Keywords: X-ray diffraction (XRD), Fourier Transform Infra-Red Spectroscopy (FTIR), Photoluminescence (PL), CIE Chromaticity Diagram, Thermo-luminescence (TL) and $Ba_2MgSi_2O_7$: Eu^{2+}, Dy^{3+}

1. Introduction
Alkaline earth silicates [AESs] were widely utilized as luminescent hosts since they possess stable crystal structure, high physical and chemical stability [1]. Many material scientists and researchers have worked on various silicate phosphors likewise $Ba_2MgSi_2O_7$:Eu^{2+}, Dy^{3+} [2], Sr_2SiO_4:Dy^{3+} [3]. $Ca_2MgSi_2O_7$:Eu^{2+}, Dy^{3+} [4]. In recent years, light-emitting diodes (LEDs) used in solid-state lighting applications, have attracted remarkable attention. From a practical point of view, LEDs-based white-light sources are superior to traditional incandescent and fluorescent lamps. LEDs based devices have higher power efficiency, energy saving, longer lifetime, reliability, safety and eco-friendly features [5-9]. $Ba_2MgSi_2O_7$:Eu^{2+} phosphor with luminescence spectrum (λ_{max} = 505 nm) are ideal for the human eye making the materials very appropriate to practical applications [10]. The location of the 4f and 5d levels of the Eu^{2+} ion and the other R^{3+}/R^{2+} ions in the host band structure are of interest, because they can, at least in principle, be used to verify the ability of the rare earth ions to trap electrons/holes [11]. The host material crystallizes in a monoclinic structure with space group C2/c (No. 15) [12]. The do-pant Eu^{2+} ions are supposed to substitute into Ba^{2+} sites in view of the similar ionic radii of the two ions, and give rise to the green luminescence as a result of the electric dipole-allowed transition from the lowest level of the excited $4f^6$ 5d configuration to the $4f^7$ ($^8S_{7/2}$) ground state [13]. Rare earth [RE] doped alkaline, alkaline earth, transition metals are called to present thermo-luminescent features when exposed to ionizing radiation [14]. The substances exhibiting TL properties are very useful in medical applications, dating, dosimetry etc. [15].
This work is aimed at an assessment of structural, optical and thermal properties of $Ba_2MgSi_2O_7$:Eu^{2+}, Dy^{3+} phosphor. In order to understand the overall mechanism, the XRD, FTIR, PL spectra, TL glow curve, and CIE chromaticity diagram were investigated.

2. Experimental studies
2.1 Sample preparation
In our study, the prepared samples with stoichiometric ratio of $Ba_2MgSi_2O_7$:Eu^{2+}, Dy^{3+} were synthesized via combustion synthesis route. Initially, all raw reagents such as Ba $(NO_3)_2$

(99.99%), Mg $(NO_3)_2$ (99.99%), SiO_2*H_2O (99.99%), and H_3BO_3 (99.99%) of Hi-media (AR grade) and Eu $(NO_3)_3$ (99.99%) and Dy $(NO_3)_3$ (99.99%) were used. Very little amount of boric acid [H_3BO_3 (99.99%)] was used as a flux. Urea (NH_2CONH_2) used as a combustion fuel. The precursor powders were mixed thoroughly with the help of very little amount of acetone (CH_3COCH_3) for 2 hour before being transferred to a cylindrical silica crucible. Then the mixture was fired at 650°C in muffle furnace. The entire combustion process was completed in about 5 min. The mixture undergoes thermal dehydration and ignites at 1000^0C for 1h in a weak reducing atmosphere with liberation of gaseous products, to yield silicates. The weak reducing atmospheres are produced by using activated charcoal and the final product was obtained with applying additional grinding into a fine powder. The resulting sample was restored in airtight bottle for characterization studies.

The chemical reaction of this process is given as follows:

Ba $(NO_3)_2$ + Mg $(NO_3)_2$ + SiO_2*H_2O + NH_2CONH_2 + Dy $(NO_3)_3$ + Eu $(NO_3)_3$ → $Ba_2MgSi_2O_7:Eu^{2+}$, Dy^{3+} + H_2O (↑) + CO_2 (↑) + N_2 (↑) (1)

Metal nitrates as oxidizers and urea is also employed as a fuel. Stoichiometric compositions of all metal nitrates and fuel are calculated based in propellant chemistry. Thus, the heat of combustion is maximum for Oxidizer/Fuel ratio 1 [16].

2.2 Sample characterization

XRD study of the crystalline structure, size and phase composition of the synthesized phosphor were noted with the help of Bruker D8 advance X-ray diffractometer with Cu-K_α radiation having wavelength (λ = 1.5406 Å, at 40 kV, 40 mA), respectively. Actual formation of this phosphor was obtained through FTIR. An FTIR spectrum was recorded with the help of Bruker Alpha Fourier transform Infra-red Spectroscopy. In photoluminescence spectra (PL), emission spectra were recorded by a spectrofluorophotometer (SHIMADZU, RF-5301 PC) using a xenon lamp of power 150 watt as excitation source [17]. A routine Thermo-luminescence (TL) study of the UV-irradiated (254 nm) samples was recorded with the help of routine TL set-up Nucleonix TLD reader with constant heating rate 5 $^oCs^{-1}$ [18]. All experiments were performed in identical conditions and it was observed that the results were reproducible. All measurements recorded at the room temperature.

3. Results and Discussions

3.1 XRD analysis

Phase identification of pure $Ba_2MgSi_2O_7$: Eu^{2+}, Dy^{3+} phosphor was done by XRD technique. Its data recorded in the range (10^0\2θ\$80^0$). Figure 1 shows the XRD pattern of this phosphor. XRD pattern of monoclinic crystal structure with a chemical formation of this phosphor is determined to be well matched with the standard data (JCPDS file No. 23-0842) [19]. The cell volume V= 711 $(Å)^3$ and the following lattice parameters: a = 8.4128 Å, b = 10.7101 Å, c = 8.4387 Å and $\alpha=90^0$, β = 110.71° $\gamma=90^0$ were also observed [10]. All parameters have been displayed in table 1.

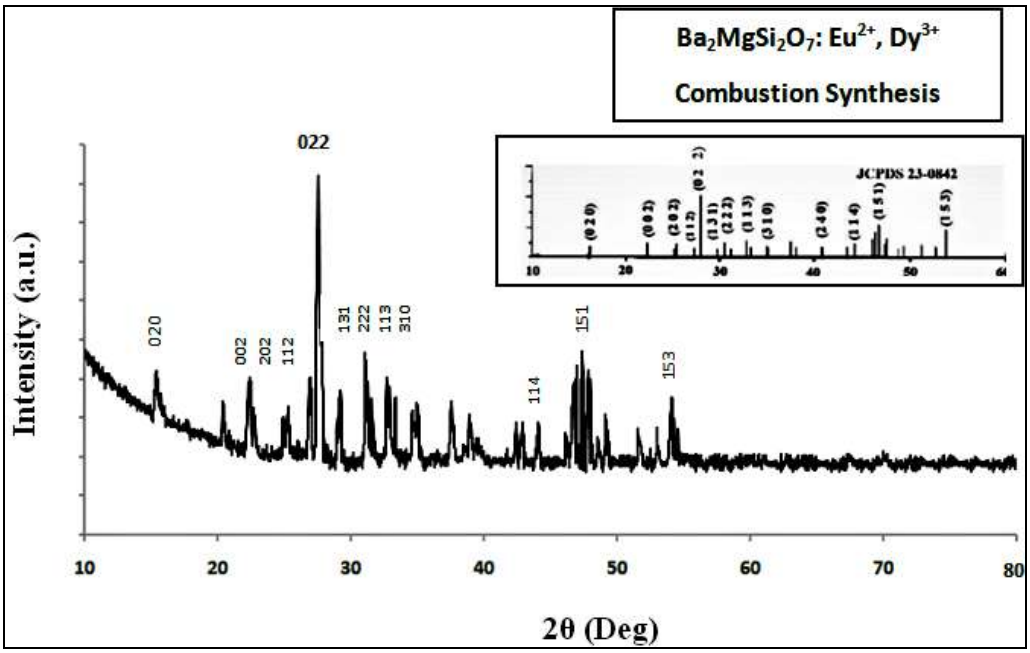

Fig 1: XRD Pattern of $Ba_2MgSi_2O_7:Eu^{2+}$, Dy^{3+} Phosphor

Table 1: According to prominent peak (211), position of the peak of the XRD patterns and the calculated value of parameters

Parameters	Ba_2MgSi_2O,: Eu^{2-}, Dy^{3-} Phosphor
Crystal Structure	Monoclinic
Space Group	C2/c
Lattice Parameters	a = 8.4182 Å, b = 103217 Å, c = 8.4313 Å, a=90° 8=110.71°, y= 90°
Crystallite Size D(nm)	29.10nm
2Theta (Deg)	27.49
Cell Volume	V=711 $(Å)^3$
Crystal Plane spacing d(Å)	3.24268Å

3.1.2 Strain Determination by Uniform Deformation Model (UDM)

The strain induced broadening in the powder material was calculated via the following formula given as below

$\varepsilon = \beta/4\tan\theta$

The strain is also calculated as 0.30.

3.2 FTIR Spectra

A FTIR spectrum of this phosphor has been shown in Figure 2. The band, allocated at 485.15, 577.68, 621.37, 677.38, 838.54, 845.28 and 1021.86 cm^{-1} can be situated to the clearly evidence of SiO_4 group. According to Gou *et al.* [20] the absorption bands, posited at 677.38 and 577.68 cm^{-1}, respectively could be assigned to the presence of SiO_4 group. In the observed IR spectrum the absorption bands of silicate groups were clearly evident. The intense band allocated at 838.54, 845.28 and 1021.86 cm^{-1} was assigned to the SiO-Si asymmetric stretch, the bands at 621.37, 677.38 cm^{-1} may be allocated to the Si-O symmetric stretch and Ba-O bending vibrations. The bands at 485.15 and 577.68 cm^{-1} are assigned to the Si-O-Si vibrational mode of bending. Peak obtained at 836 cm^{-1} can also be allocated to Mg-O bending vibrations [21-24].

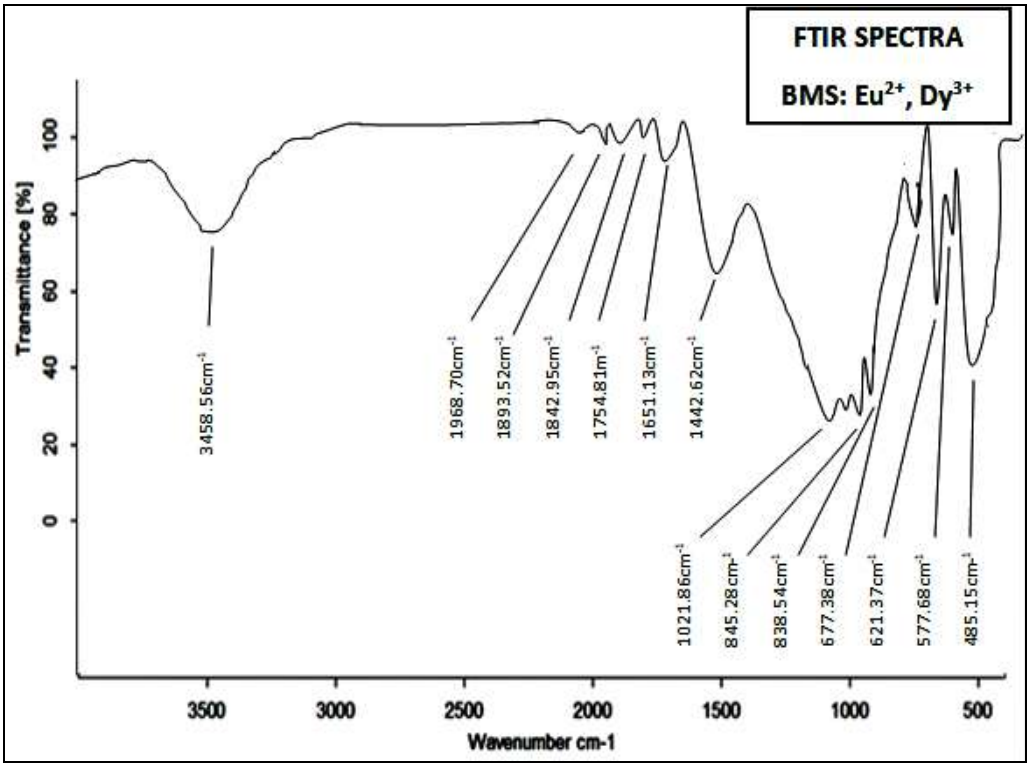

Fig 2: FTIR Spectra of $Ba_2MgSi_2O_7$: Eu^{2+}, Dy^{3+} phosphor

The free CO_3^{2-} ion has a D3h symmetry 69 (trigonal planar) and its spectrum is dominated by the band (asymmetric stretching) at 1651.13cm^{-1}. The bands allocated at 1754.81, 1842.52, 1893.52 and 1968.70 cm^{-1} are allocated to carbonation processes. Europium [Eu^{2+}] ions are expected to substitute Ba^{2+} sites because the coordination number of Ba^{2+} ion is eight and that for Mg^{2+} ions and Si^{4+} ions is four. It's hard for Eu^{2+} ions to incorporate the tetrahedral [MgO_4] or [SiO_4] symmetry but it can easily incorporate octahedral [BaO_8] [25]. This might produce distortion in the lattice resulting in 1400 and 1650 cm^{-1} vibration modes assigned to vibration in Ba^{2+} and Mg^{2+} ions respectively [26]. Various peaks in the range of 1800-1900 cm^{-1} are possibly because of Ba-O stretching. Two peaks situated at 3458.56 cm^{-1} are visible because of stretching of O-H functional group which supports the presence of moisture in the sample.

3.3 Photoluminescence properties

The excitation and emission spectra of $Ba_2MgSi_2O_7$: Eu^{2+}, Dy^{3+} phosphors prepared were shown in Figure 3. The excitation spectrum was monitored at a wavelength of 520 nm which displays a prominent peak at 395 nm and another peak is situated at 346 nm wavelength. The emission spectra are identical in shape and the bands differ only in intensities. The broadband emission spectra centered at 520 nm (Green region) observed under the UV excitation of 395 nm correspond to the Eu^{2+} emission arising due to transitions from sublevels of $4f^6\ 5d^1$ configuration to $^8S_{7/2}$ level of the $4f^7$ configuration but with Eu^{2+} occupying different lattice sites. The emission spectra cover 400 nm to 600 nm which is a sign of a very good phosphor. Since the crystal field can greatly affect the $4f^6\ 5d^1$ electron states of Eu^{2+}, it suggests that the crystal field is not changed much with the compositional variation [27-29]. Eu^{2+} ions are expected to replace Ba^{2+} sites because the coordination number of Ba^{2+} ion is eight and that for Mg^{2+} ions and Si^{4+} ions is four. It's hard for Eu^{2+} ions to incorporate the tetrahedral [MgO_4] or [SiO_4] symmetry but it can easily incorporate octahedral [BaO8] illustrated in Figure 3 [30].

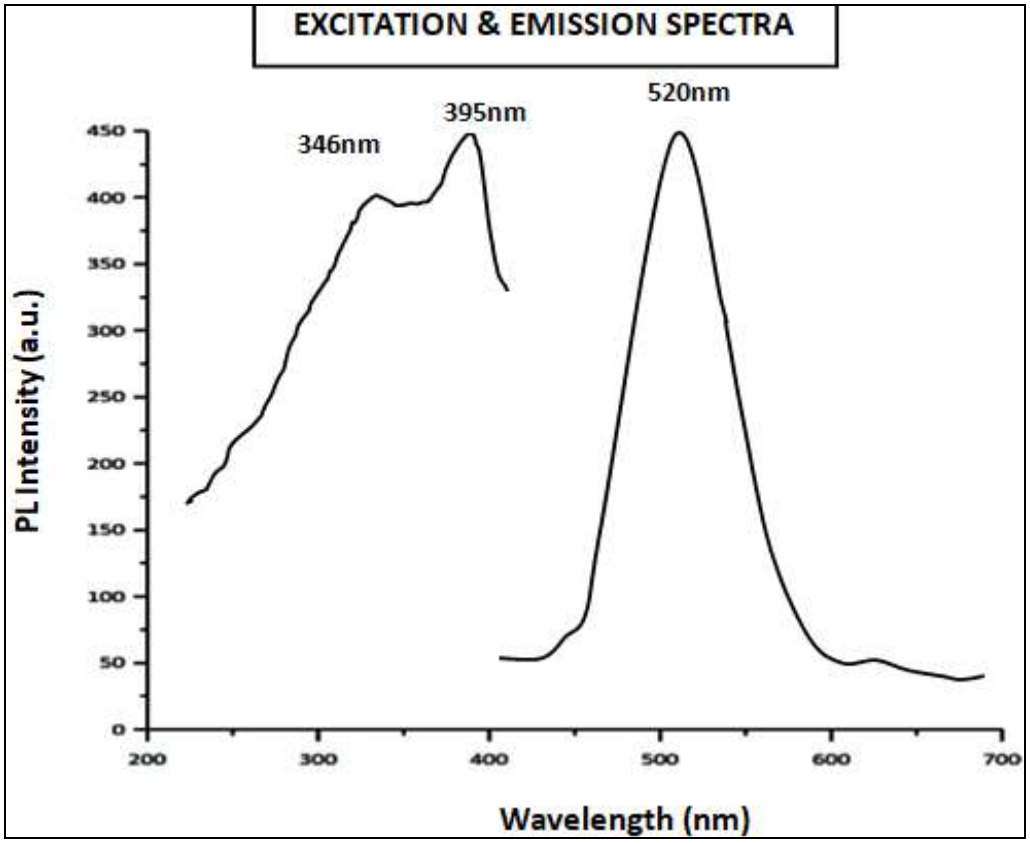

Fig 3: Excitation and Emission Spectra of $Ba_2MgSi_2O_7$: Eu^{2+}, Dy^{3+} Phosphor

Table 2: Concentrations of Rare Earths (In mol %)

Concentrations of Rare Earths (In mol %)		
Phosphor	**Eu^{2+} (Doping)**	**Dy^{3+} (Co-Doping)**
$Ba2MgSi_2O_7$:Eu^{2+}, Dy^{3+}	0.5	2

3.4 CIE chromaticity diagram

Fig. 4 shows the CIE diagram and the chromaticity coordinates of the $Ba_2MgSi_2O_7$:Eu^{2+}, Dy^{3+} phosphor. The calculated chromaticity coordinates for the green light emitted from $Ba_2MgSi_2O_7$:Eu^{2+}, Dy^{3+} phosphor is given by (X = 0.2527, Y = 0.6125) [31].

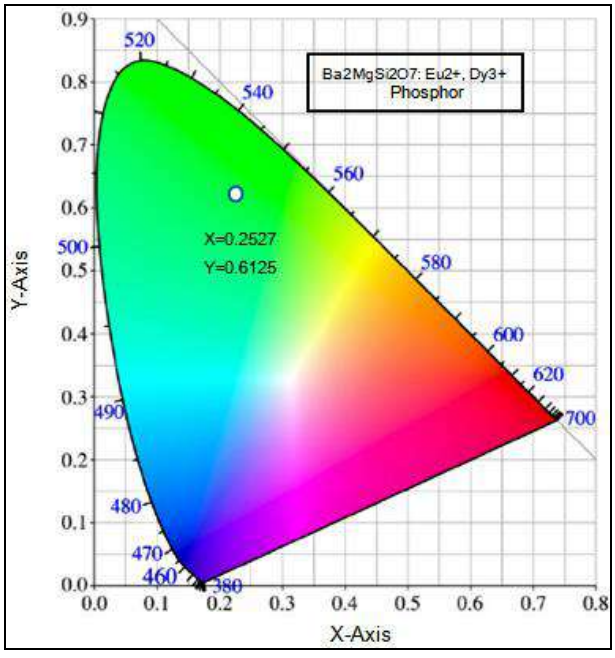

Fig 4: CIE Chromaticity Diagram

3.5 Thermo-luminescence properties

TL materials do not emit light, if it is not exposed by some ionizing radiations. TL properties of the phosphors are strongly dependent on traps created by the lattice defects [32]. Fig: 6 displays TL glow curve of the sample for 15 min UV exposure. Thermo-luminescence signal is optimum for 15 minutes of UV exposure, after that it starts to decrease. The charge carrier density may have been increasing with increasing UV exposure, but after 15 minutes of UV exposure. Trap level may have started to destroy resulting in decrease in TL signals. The TL glow curves (Fig: 6) exhibit a broad peak because of the transition between ground and excited energy levels of the do-pant Eu^{2+}. The value of shape factor obtained between the ranges from 0.49-0.54, which signs the second order kinetics that supports the probability of retrapping released charge carriers before recombination. The afterglow of any phosphor is generated by the de-trapped carriers which recombine with the opposite carriers in the luminescent center with a transition resulting in visible region [33-34].

3.6 Calculation of kinetic parameters

The TL glow curve of a phosphor mainly depends on the kinetic parameters which include [Trap Depth or Activation Energy E], [Frequency Factor s] and [Order of Kinetics b].

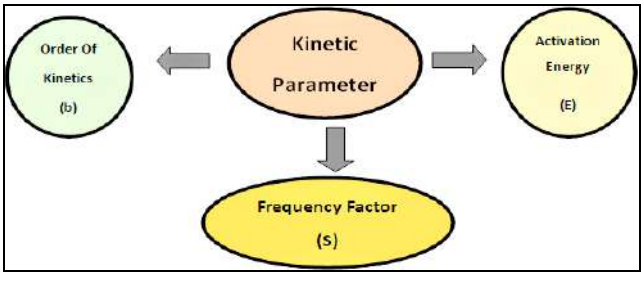

Fig 5: Types of Kinetic Parameters

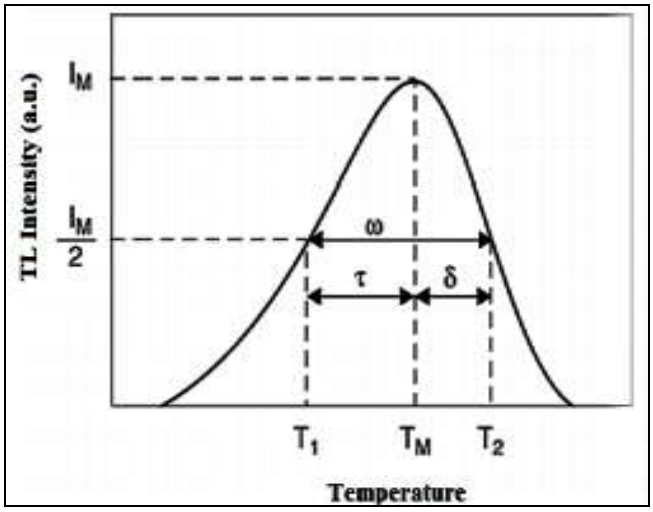

Fig 6: Schematic Diagram of Glow Curve Peak Shape Method

3.6.1 Order of Kinetics [b]

The kinetic order for glow peak of $Ca_2MgSi_2O_7:Eu^{2+}$ phosphor can be determined via calculating geometrical factor μ_g from the mathematical relation as follows:

$$\mu_g = \delta/\omega = T_2 - T_m/T_2 - T_1 \quad (2)$$

where T_m is the optimum peak temperature, T_1 and T_2 are temperatures at half intensity on the ascending and descending parts of the glow peak, respectively, [$\omega = T_2 - T_1$], the high-temperature half width [$\delta = T_2 - T_m$]. The geometric factor is to differentiate between first and second order TL glow peak. [μ_g = 0.39-0.42] for the first order kinetics; [μ_g = 0.49-0.52] for the second order kinetics and [μ_g = 0.43-0.48] for the mixed order kinetics [39].

3.6.2 Activation energy (E)

The activation energy [E] or trap depth can be determined by the general formula, which is valid for any kinetics. It is given by mathematical relation as follows [39]:

$$E = C_\alpha\left(\frac{kT_m^2}{\alpha}\right) - b_\alpha(2kT_m) \quad (3)$$

For general order kinetics, the values of the C_α and b_α ($\alpha = \tau, \delta, \omega$) are expressed as $c_\tau = [1.51 + 3(\mu_g - 4.2)$, $b_\tau = [1.58 + 0.42((\mu_g - 0.42)]$; $c_\delta = [0.976 + 7.3(\mu_g - 0.42)]$, $b_\delta = 0$ and $c_\omega = [2.52 + 10.2(\mu_g - 0.42)]$, $b_\omega = 1.0$.

3.6.3 Frequency factor

It's clearly reflects the probability of electron escape from the traps after exposure to ionizing radiation. Frequency factor is one of the most significant parameters for material characterization. After obtaining the order of kinetics [b] and activation energy [E], the frequency factor [s] can be determined with the help of the following mathematical relation through replacing the values of E and b:

$$\frac{\beta E}{kT_m^2} = s\left[1 + (b-1)\frac{2kT_m}{E}\right]\exp\left(-\frac{E}{kT_m}\right) \quad (4)$$

Where k is Boltzmann constant, E is activation energy, b is an order of kinetics, T_m is a temperature of peak position, and β is the heating rate. In the present work $\beta = 5^0Cs^{-1}$ [35-36].

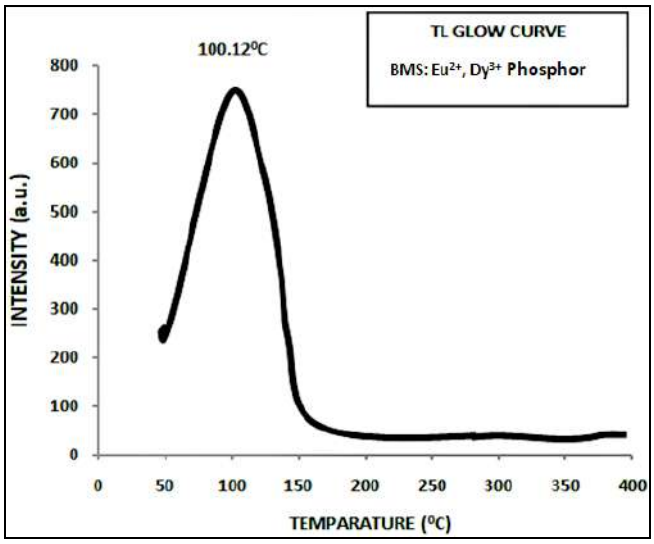

Fig 7: TL Glow Curve of $Ba_2MgSi_2O_7:Eu^{2+}$, Dy^{3+} phosphor

The effect of 15min UV exposure on this phosphor and its different TL parameters are calculated [Table no. 3]. In our TL experimental case, geometric shape factor (μ_g) is calculated as 0.49. The value of geometric shape factor indicates that it is a case of second order kinetic, due to, it is also responsible for deeper trap depth.

Table 3: Kinetic Parameters

No.	Name of Phosphor	UV min	HTR	T_1 °C	T_m °C	T_2 °C	τ	δ	ω	$\mu=\delta/\omega$	E (eV)	Frequency Factor (s^{-1})
1.	BMS: Eu^{2+},Dy^{3+}	15	5	72.67	100.12	126.79	27.45	26.67	54.12	0.49	0.62	1.03×10^7

Observing the TL glow curve, we find that the maximum glow curve is obtained at 100.12 °C. From 50.16 °C temperature, TL intensity is continuously increasing up to 100.12 °C, respectively. There after that the TL intensity is decreasing continuously up to 151.42 °C and their after TL intensity curve is near about flate and constant having the lowest value of TL intensity up to 400 °C. Sakai *et al*. and Mashangva *et al*. were reported that an appropriate trap depth (0.65-0.75 eV) is necessary for materials to display long persistence characteristics [37-38]. So, the trap density of synthesized materials is appropriate for long afterglow properties. In our case of phosphor, the geometric factor/ shape factor (μ_g) is obtained 0.49 and activation energy is found 0.62 eV respectively, which indicates of a considerable persistency.

4. Conclusion

$Ba_2MgSi_2O_7:Eu^{2+}$, Dy^{3+} phosphor was prepared via combustion synthesis route. The identified phase structure was monoclinic structure with a space group C2/c which is

confirmed through JCPDS # 23-0842. The average crystallite size (D) is calculated as 29.10nm and lattice strain as 0.30 respectively. The actual phase formation and identification of functional group has been clarified with the help of FTIR spectroscopy. The broadband emission spectra centered at 520 nm (Green region) observed under the ultraviolet excitation of 395 nm correspond to the Eu^{2+} emission arising due to transitions from sublevels of $4f^6 5d^1$ configuration to $^8S_{7/2}$ level of the $4f^7$ configuration but with Eu^{2+} occupying different lattice sites. TL glow curve of this phosphor with 15min UV irradiation time at constant heating rate 5 $^oCs^{-1}$. The single TL glow curve peak was allocated at 100.12^{o}C temperature respectively, and these peak positions remains constant with UV irradiation time. The phosphors synthesized by combustion synthesis route which good supports the fact that the phosphor show considerable amount of persistency in its luminescence property.

5. Acknowledgements

We gratefully acknowledge the kind support for the facility of XRD analysis Dept. of Metallurgical Engineering and FTIR analysis Dept. of physics, NIT Raipur (C.G.). Authors are also thankful to Dept. of physics, Pt. Ravishankar Shukla University, Raipur (C.G.) for providing us the facility of Photoluminescence (PL) and Thermo-luminescence (TL) analysis. We are also heartily grateful to Dept. of physics, Dr. Radha Bai, Govt. Navin Girls College Mathpara Raipur (C.G.), providing the facility of muffle furnace and other essential research equipments.

6. References

1. Craford MG. Proc. SPIE 4776 2002.
2. Gupta SK, Kumar M, Natarajan V, Godbole SV. Optical properties of sol-gel derived Sr_2SiO_4:Dy^{3+}-Photo and thermally stimulated luminescence. Journal Optical Material 2013;35(12):2320-8.
3. Aitasalo T, Hölsä J, Laamanen T, Lastusaari M, Lehto L, Niittykoski J *et al*. 2006;23:481-486.
4. Sharma S, Dubey SK, Diwakar AK, Pandey S. Novel white light emitting ($Ca_2MgSi_2O_7$:Dy^{3+}) Phosphor. Journal of materials science research and reviews 2021;8(4):164-171.
5. Kim JS, Jeon PE, Choi JC, Park HL, Mho SI, Kim GC *et al*. Warm-white-light emitting diode utilizing a single-phase full-color $Ba_3MgSi_2O_8$:Eu^{2+}, Mn^{2+} phosphor Appl, Phys. Lett 2004;84:2931-2933.
6. Zukauskas A, Shur MS, Gaska R. Introduction to Solid-State Lighting, Wiley Interscience, New York 2002. ISBN 978-0-471-21574-5.
7. Kim JS, Park YH, Choi JC, Park HL, Kim GC, Yoo JH. Color tunability of nanophosphors by changing cations for solid-state lighting, Solid State Commun 2006;137:187-190.
8. Schubert EF, Kim JK. Solid-state light sources getting smart, Science 2005;308:1274-1278.
9. Neeraj S, Kijima N, Cheetham AK. Novel red phosphors for solid-state lighting: the system $NaM(WO_4)_2$−$x(MoO_4)x$:Eu^{3+} (M = Gd, Y, Bi), Chem. Phys. Lett. 2004;387:2-6.
10. Aitasalo T, Hreniak D, Holsa J, Laamanen T, Lastusaari M, Nittykoski J *et al*. Persistent luminescence of $Ba_2MgSi_2O_7$:Eu^{2+}. J Lumin 2007, 122-123, 110-112.
11. Hölsäa J, Niittykoskia J, Kirmb M, Laamanena T, Lastusaaria CM, Novakd P *et al*. Synchrotron Radiation Study of the $M_2MgSi_2O_7$:Eu^{2+} Persistent Luminescence Materials. ECS Transactions 2008;6(27):1-10. 10.1149/1.2938743.
12. Aitasalo T, Hölsä J, Laamanen T, Lastusaari M, Lehto L, Niittykoski J *et al*. 2006;23:481.
13. Jing Yan, Lixin Ning, Yucheng Huang, Chunmeng Liu, Dejian Hou, Bingbing Zhang *et al*. Luminescence and electronic properties of $Ba_2MgSi_2O_7$: Eu^{2+}: A combined experimental and hybrid density functional theory study. Journal of Materials Chemistry C.
14. Shionoya S, Yen WM. Phosphor Handbook, CRC press, New York, 1998.
15. Watanabe S, Cano NF, Carmo LS, Barbosa RF, Chubaci JFD. Radiation Measurements 2015;72:66.
16. Kingsely JJ, Patil KC. Material letters. 1988; 6:427.
17. Sharma S, Dubey SK, Diwakar AK, Pandey S. Novel white light emitting ($Ca_2MgSi_2O_7$:Dy^{3+}) Phosphor. Journal of Materials Science Research and Reviews. 2021; 8(4):164-171.
18. Shashank Sharma, Sanjay Kumar Dubey, Sanjay Pandey, Diwakar AK. Optical Characteristics of Novel WLED ($Ca_2MgSi_2O_7$:Dy^{3+}) Phosphor. North Asian International Research Journal of sciences, Engineering & I.T. (Joint Committee on Powder Diffraction Standard) JCPDS file No. 23-0842 2021, 7(11).
19. Gou Z, Chang J, Zhai W, Eur J. Ceram. Soc. 2005; 25:1507-1514.
20. Frost RL, Bouzaid JM, Reddy BJ. Vibrational spectroscopy of the sorosilicate mineral hemimorphite $Zn_4(OH)_2Si_2O_7·H_2O$. Polyhedron. 2007; 26(12):2405-12.
21. Chandrappa GT, Ghosh S, Patil KC. Synthesis and Properties of Willemite, Zn_2SiO_4, and M^{2+}:Zn_2SiO_4 (M= Co and Ni). Journal of Materials Synthesis and Processing 1999;7(5):273-9.
22. Makreski G, Jovanovski B, Kaitner A, Gajovic T, Biljan. Vib. Spectrosc 2007;44:162.
23. Caracas R, Gonze X. Ab initio determination of the ground-state properties of $Ca_2MgSi_2O_7$ åkermanite. Physical Review B 2003;68(18):184-102.
24. Komeno A, Uemastu K, Toda K, Sato M, Alloys J. Compd 2006, 408-412, 871-874.
25. Salim MA, Hussin R, Abdullah MS, Abdullah S, Alias NS, Fuzi SAA *et al*., Solid State Science and echnology 2009;17(2):59-64.
26. Shi C, Fu Y, Liu B, Zhang G, Chen Y, Qi Z *et al.*, J Lumin 2007, 122-123, 11-13.
27. Aitasalo T, Hölsä J, Laamanen T, Lastusaari M, Lehto L, Niittykoski *et al*. 2006;23:481-486.
28. Komeno A, Uemastu K, Toda K, Sato M. VUV properties of Eu-doped alkaline earth magnesium silicate J Alloys Compd 2006, 408-412, 871-874.
29. Ardit M, Zanelli C, Dondi M, Cruciani G. Periodico di Mineralogia 2011;80:155-165.
30. CIE. International Commission on Illumination. Publication CIE no. 15 (E-1.3.1) 1931.
31. Yuan Z, Chang C, Mao D, Ying W. Effect of composition on the luminescent properties of $Sr_4Al_{14}O_{25}$: Eu^{2+}, Dy^{3+} phosphors. J Alloys Compd 2004;377(1-2):268-71.
32. Chen T, McKeever S. Theory of Thermo-luminescence and Related Phenomena World Scientific Publishing Co. Pvt. Ltd 1997.

33. Kaur J, Shrivastava R, Dubey V, Jaykumar B. Res. Chem. Intermed 2012. DOI 10.1007/s11164-013-1112-5.
34. Chen R, Mckeever SWS. Theory of Thermo-luminescence and Related Phenomenon, World Scientific Press, Singapore 1997.
35. Mckeever SWS. Thermo-luminescence of Solids, Cambridge University Press, Cambridge 1985.
36. Mashangva M, Singh MN, Singh B. Indian J Pure Appl. Phys 2011;49:583-589.
37. Sakai R, Katsumata T, Komuro S, Morikawa T, Lumin J 1999;85:149-154.
38. Shashank Sharma, Sanjay Kumar Dubey, Diwakar AK. Thermo-luminescence properties of Host $Ca_2MgSi_2O_7$ Phosphor. IRJMETS 2021, 3(11).